RELIABILITY BASED DESIGN OPTIMIZATION FOR MULTIAXIAL FATIGUE DAMAGE ANALYSIS USING ROBUST HYBRID METHOD

A. Yaich*

Laboratory of Mechanics, Modeling and Manufacturing
National School of Engineers of Sfax
Sfax, Tunisia

Laboratory of Optimization and Reliability in Structural Mechanics
Normandie Université
INSA of Rouen
Rouen, France

G. Kharmanda

Biomedical Engineering Department
Lund University
Lund, Sweden

A. El Hami

Laboratory of Optimization and Reliability in Structural Mechanics
Normandie University
INSA of Rouen
Rouen, France

L. Walha **M. Haddar**

Laboratory of Mechanics, Modeling and Manufacturing
National School of Engineers of Sfax
Sfax, Tunisia

ABSTRACT

The purpose of the Reliability-Based Design Optimization (RBDO) is to find the best compromise between safety and cost. Therefore, several methods, such as the Hybrid Method (HM) and the Optimum Safety Factor (OSF) method, are developed to achieve this purpose. However, these methods have been applied only on static cases and some special dynamic ones. But, in real mechanical applications, structures are subject to random vibrations and these vibrations can cause a fatigue damage. So, in this paper, we propose an extension of these methods in the case of structures under random vibrations and then demonstrate their efficiency. Also, a Robust Hybrid Method (RHM) is then developed to overcome the difficulties of the classical one. A numerical application is then used to present the advantages of the modified hybrid method for treating problem of structures subject to random vibration considering fatigue damage.

Keywords: Reliability Based Design Optimization, Multiaxial fatigue damage, Robust Hybrid Method, Random vibrations.

1. INTRODUCTION

In our daily life, many structures are subject to random vibrations. These vibrations can cause a fatigue damage. In the last few decades, and in order to estimate a life time of a structure subject to random loads, many studies have been elaborated. For multiaxial fatigue damage case, the structure's life time can be estimated by considering many criteria that calculate the fatigue damage. Such criteria can be mathematically represented by:

$$g(S_{i,j}(t), T) \leq 1 \tag{1}$$

* Corresponding author (ahmed.yaich@insa-rouen.fr)

DOI : 10.1017/jmech.2017.44
Copyright © 2017 The Society of Theoretical and Applied Mechanics
https://doi.org/10.1017/jmech.2017.44 Published online by Cambridge University Press

Where $S_{i,j}(t)$ is the stress tensor at any given location in the structure and for any time $t \in [0, T]$ A fatigue crack can appear if the inequality (1) is not satisfied at any point of the structure.

In order to reduce the computing time, the fatigue damage analyses have been carried out in the frequency domain. This can be seen in previous works such as Pitoiset [1-2] which defined a formulation of Matake's criterion and Crossland's Criterion in frequency domain. According to Weber *et al*. [3] and Wu *et al*. [4], the Sines criterion seems to give the best evaluation of damage subject to random stresses.

Let's consider a linear structure subject to stationary ergodic Gaussian loads. According to Pitoiset [5], the crack will not initiate before a certain number of repetitions Ne of the periodic random load of duration T if the average of the damage should not exceed the fatigue limit.

$$E[g(S_{i,j}(t),T)] \le 1 \tag{2}$$

Then, to calculate the average of the damage in the frequency domain, we need to calculate the Power Spectral Densities (PSD) of the stresses for all point in the structure. The spectral matrix is obtained by the Fourier transformation of the correlation functions of the stresses [6].

In the last few decades, designers seek to minimize the cost of a mechanical part considering a given level of reliability. The objective of the Reliability Based Design Optimization is to design structures that should be both reliable and economical.

In the Deterministic Design Optimization (DDO) [7-8], the aim of the designer is to reduce the design's cost without considering the effects of uncertainties concerning geometry, materials and loading. The optimal solution resulted from the optimization process may then lead to an inappropriate reliability level. On the other side, the objective of the Reliability-Based Design Optimization (RBDO) is to minimize the structural weight to provide an improved design with a high level of confidence.

In this context, several methods have been treated to solve the RBDO problem. These approaches can be classified into three groups: the two-level approach, the single loop approach and the decoupled approach. Those methods are used in different domains such as civil engineering [9], mechatronic [10], vibro-acoustic [11], … Aoues and Chateauneuf [12] tested a various RBDO approaches in a benchmark constituted of four examples. In fact, these approaches can be carried out in two separated spaces: physical space and normalized space. To this end, the optimization problem requires considerable computation time.

In order to improve the numerical performance, Kharmanda *et al*. [13-15] have elaborated an efficient method called Hybrid Method (HM). This method consists in solving simultaneously the optimization problem and the reliability problem. The solution is carried out in the Hybrid Design Space (HSD) which is contain the deterministic and the random variables and it can satisfy a specific reliability level.

This method has successfully reduced the computing time but the RBDO problem become more complex than the DDO problem. Therefore, another methodology called Optimum Safety Factor (OSF) has been elaborated [16-17]. Using this method, the optimal solution is obtained by considering the design point and the computed safety factors which are calculated from the derivative of the constraint function.

The efficiency of these methods has demonstrated only considering static cases and some special dynamic ones. In this paper, an application of these methods is carried out on structures submitted to multiaxial random vibrations and next a Robust Hybrid Method (RHM) is proposed. The efficiency of the new method is finally demonstrated considering a numerical application on an example of structure under random vibrations.

2. MULTIAXIAL FATIGUE DAMAGE ANALYSIS UNDER RANDOM VIBRATIONS

2.1 Formulations and Developments

The main purpose of multiaxial fatigue criteria is to determine the location of the critical point in a structure. It can be assumed, by many author, that the crack initiation is governed by the second invariant of the deviator stress tensor [18-19]. This can be seen in the Crossland criterion (Eq. (3)) and Sines Criterion (Eq. (4)) where $J_{2,a}$ is the second invariant of the deviator stress tensor.

$$D_{Crossland} = \frac{\sqrt{J_{2,a}} + A \max\limits_{0 \le t \le T}\{p(t)\}}{B} \le 1 \tag{3}$$

$$D_{Sines} = \frac{\sqrt{J_{2,a}} + A\,E[p(t)]}{B} \le 1 \tag{4}$$

Where $p(t)$ is hydrostatic pressure which is determined by the normal stresses components S_{xx}, S_{yy} and S_{zz} of the stress tensor S_{ij} (Eq. 5) and A, B are constants related with the material. For the Sines criterion, they are defined by the endurance limit in alternating traction f_{-1}, the endurance limit in alternating torsion t_{-1} and the breaking strength R_m (Eq. (6-7)).

$$p(t) = \frac{1}{3} Trace\{S_{ij}\} = \frac{1}{3}(S_{xx} + S_{yy} + S_{zz}) \tag{5}$$

$$A = \frac{3t_{-1}(R_m + f_{-1})}{f_{-1}R_m} - \sqrt{6} \tag{6}$$

$$B = t_{-1} \tag{7}$$

It can be noted that the Crossland criterion need the calculation of maximum of the hydrostatic pressure while the Sines criterion use it's mean. This reduces the calculation time of the damage if it's calculated by the Sines criterion and have almost the same result such the Crossland criterion [20].

Let's consider now a linear structure subject to stationary ergodic Gaussian loads. According to Eq. (2), the crack will not initiate before Ne repetitions of the

https://doi.org/10.1017/jmech.2017.44 Published online by Cambridge University Press

periodic random load of duration T if the average of the damage should not exceed the fatigue limit. The Sines criterion is then defined by:

$$E[D_{Sines}] = \frac{E[\sqrt{J_{2,a}}] + A\,E[p(t)]}{B} \leq 1 \qquad (8)$$

The problem now is the determination of the average of the shear stress amplitude $E[\sqrt{J_{2,a}}]$. In fact, for a proportional loading, $\sqrt{J_{2,a}}$ can be defined by the Eq. (9).

$$\sqrt{J_{2,a}} = \sqrt{\frac{1}{6}[(S_{xx,a}-S_{yy,a})^2 + (S_{yy,a}-S_{zz,a})^2 + (S_{zz,a}-S_{xx,a})^2 + 6(S_{xy,a}-S_{yz,a}-S_{xz,a})^2]} \qquad (9)$$

In this expression, the alternating component of stress $S_{ij,a}$ is defined by:

$$S_{ij,a} = \frac{1}{2}(\max_{0\leq t\leq T}[S_{ij}(t)] - \min_{0\leq t\leq T}[S_{ij}(t)]); \quad i,j = x,y,z \qquad (10)$$

Note that the $\sqrt{J_2(t)}$ corresponds to the square root of the second invariant of the deviatoric stress tensor. So, to simplify the calculation and for further development, it is important to relate it to a norm in a five-dimensional Euclidean space E5 [21]. By Noting $\|\cdot\|$ the Euclidian norm, we have:

$$\sqrt{J_{2,a}} = \sqrt{D_{1,a}^2 + D_{2,a}^2 + D_{3,a}^2 + D_{4,a}^2 + D_{5,a}^2} = \|d_a\| \qquad (11)$$

Where:

$$d = \begin{cases} D_1 = \frac{\sqrt{3}}{2}\left(\frac{2}{3}S_{xx} - \frac{1}{3}S_{yy} - \frac{1}{3}S_{zz}\right) \\ D_2 = \frac{1}{2}(S_{yy} - S_{zz}) \\ D_3 = S_{xy} \\ D_4 = S_{yz} \\ D_5 = S_{xz} \end{cases}$$

i.e.

$$d(t) = P.s(t) \qquad (12)$$

With $d = [D_1, D_2, D_3, D_4, D_5]^T$, $s = [S_{xx}, S_{yy}, S_{zz}, S_{xy}, S_{yz}, S_{xz}]^T$ and

$$P = \begin{bmatrix} \frac{\sqrt{3}}{3} & -\frac{\sqrt{3}}{6} & -\frac{\sqrt{3}}{6} & 0 & 0 & 0 \\ 0 & \frac{1}{2} & -\frac{1}{2} & 0 & 0 & 0 \\ 0 & 0 & 0 & 1 & 0 & 0 \\ 0 & 0 & 0 & 0 & 1 & 0 \\ 0 & 0 & 0 & 0 & 0 & 1 \end{bmatrix}$$

For a non-proportional load, the expression (10) is not available. For this reason, many approaches have been proposed in order to determine $\sqrt{J_{2,a}}$ such as Bin Li [22], Balthazar J. C. [23] and Bernasconi A. [24]. These definitions are confronted with experimental results in [25-29].

Bin Li & al. [22] propose to consider the smallest ellipse of the semi-axes R_1 and R_2 circumscribing the path of $\sqrt{J_{2,a}}$ to realize the non-proportional loading. Thus, $\sqrt{J_{2,a}}$ for the non-proportional load is approached by $\sqrt{J_{2,a}} = \sqrt{R_1^2 + R_2^2}$.

With the same principle, and to determine of the equivalent shear stress amplitude, we consider that the semi-axes R_1, R_2, R_3, R_4 and R_5 of the five-dimension ellipsoid circumscribed to the loading path of $\sqrt{J_{2,a}}$ and oriented in its principal directions. $\sqrt{J_{2,a}}$ can then be written as well:

$$\sqrt{J_{2,a}} = \sqrt{R_1^2 + R_2^2 + R_3^2 + R_4^2 + R_5^2} \qquad (13)$$

So, for a random load, the estimation of $\sqrt{J_{2,a}}$ consist in the estimation of the semi-axes *Ri*. This is carried out by the analysis of the principal components of the covariance matrix Σ_d of *d*. It is defined by:

$$\Sigma_d = E[(d(t) - \bar{d}).(d(t) - \bar{d})^T] \qquad (14)$$

Σ_d can also be defined from the covariance matrix of the stress Σ_s as follow:

$$\Sigma_d = P\Sigma_s P^T \qquad (15)$$

The diagonal terms of Σ_d matrix present the variance of each component. However, the terms out of diagonal present the variance between each component. In general, these terms are different of zero. So Σ_d is not diagonal.

There is an orthonormal basis of eigenvectors Ad such that:

$$\Sigma_{\tilde{d}} = A_d \Sigma_d A_d^T = diag(\sigma_1^2, \sigma_2^2, \sigma_3^2, \sigma_4^2, \sigma_5^2) \qquad (16)$$

with $\sigma_1 \geq \sigma_2 \geq \sigma_3 \geq \sigma_4 \geq \sigma_5$.

Then we can define a vector $\tilde{d}$ linearly associated with d by an orthogonal transformation such as:

$$\tilde{d}(t) = A_d d(t) \qquad (17)$$

With

https://doi.org/10.1017/jmech.2017.44 Published online by Cambridge University Press

$$\tilde{d}(t)=\begin{bmatrix}\widetilde{D_1}(t)\\ \widetilde{D_2}(t)\\ \widetilde{D_3}(t)\\ \widetilde{D_4}(t)\\ \widetilde{D_5}(t)\end{bmatrix} \tag{18}$$

Since the components $\tilde{D}_t(t)$ are a Gaussian stationary process, then we can estimate the maximum value of $\tilde{D}_t(t)-\bar{\tilde{D}}_t$ by the application of the peak factor theory (Eq. (19a)). Eq. (19b) presents the peak factor theory for zero mean stationary Gaussian, random process $s(t)$ [21], [30]

$$E[\max(\tilde{D}_t(t)-\bar{\tilde{D}}_t)] \approx \sigma_i\left(\sqrt{2\ln N_p(\tilde{D}_t(t))}+\frac{0,5772}{\sqrt{2\ln N_p(\widetilde{D}_t(t))}}\right),\quad i=1\ldots5 \tag{19a}$$

$$E[\max(s)]\approx\sigma_s\left(\sqrt{2\ln N_p(s(t))}+\frac{0,5772}{\sqrt{2\ln N_p(s(t))}}\right) \tag{19b}$$

Where $N_p(\tilde{D}_t(t))$ is the average of the number of maxima which can be calculated from the spectral moment m_i of the random process $\tilde{D}_t$ (Eqs. (20-21)). $\Phi_{\tilde{D}_i}$ present the PSD of the random process $\tilde{D}_t$ and f is the frequency in *Hz*.

$$N_p=\sqrt{\frac{m_4}{m_2}} \tag{20}$$

$$m_i=\int_{-\infty}^{+\infty}|f|^i\,\Phi_{\tilde{D}_i}(f)df \tag{21}$$

Considering the concepts introduced previously, the random semi-axis of the loading can be characterized by:

$$E[R_i]=\frac{1}{2}\left[E[\max(\tilde{D}_t(t)-\bar{\tilde{D}}_t)]-E[\min(\tilde{D}_t(t)-\bar{\tilde{D}}_t)]\right] \tag{22}$$

Since they are not correlated and are assumed to be Gaussian we can consider that:

$$E[\max(\tilde{D}_t(t)-\bar{\tilde{D}}_t)]=-E[\min(\tilde{D}_t(t)-\bar{\tilde{D}}_t)] =E[R_i],\quad i=1\ldots5 \tag{23}$$

Then we have:

$$E[R_i]\approx\sigma_i\left(\sqrt{2\ln N_p(\tilde{D}_t(t))}+\frac{0,5772}{\sqrt{2\ln N_p(\widetilde{D}_t(t))}}\right) \tag{24}$$

For a stationary Gaussian random loading, we can assume that the average of $\sqrt{J_{2,a}}$ is defined by:

$$E[\sqrt{J_{2,a}}]=\sqrt{E[R_1]^2+E[R_2]^2+E[R_3]^2+E[R_4]^2+E[R_5]^2} \tag{25}$$

The damage is then can be calculated by replacing $E[\sqrt{J_{2,a}}]$ in the Eq. (8) by the expression (25).

2.2 Strategy Implementation

To summarize, the implementation of the fatigue damage analysis strategy is illustrated in Fig. 1. The algorithm consists of two subproblems: the first subproblem, is to calculate the Power Spectral Densities of the stresses. First build the model by defining the geometry, material proprieties and loads. Then, a modal analysis is necessary to determine the normal modes of the model. We conclude this first subproblem by the spectral analysis to calculate the stresses PSD at each element of the structures.

For the second subproblem, and in order to evaluate the fatigue damage, the calculated PSD are then introduced into MATLAB software to evaluate the stresses covariance Matrix as a first step. This allows us to calculate the covariance matrix Σ_d using Eqs. (14-15). The covariance matrix $\Sigma_{\tilde{d}}$ and the PSD $\Phi_{\tilde{d}}$ are obtained by the orthogonal transformation of the Σ_d matrix. Using Eqs. (20-21) the number of maxima N_p of each parameter of the vector $\tilde{d}$ is calculated. Then, the average of the shear stress amplitude $E[\sqrt{J_{2,a}}]$ is determined, using Eqs. (24-25). Finally, the fatigue damage is determined at each point of the structure using the Sine criterion.

3. RELIABILITY BASED DESIGN OPTIMIZATION OF A STRUCTURE UNDER RANDOM VIBRATIONS

3.1 Deterministic Design Optimization

The use of the DDO model in the structural design is become increasingly common with the advent of computer technology and the development of the finite element analysis software. In fact, this approach consists in assigning safety factors to constraint functions in order to integrate the presence of uncertainties in the design variables.

Using these safety factors, the optimization problem consists then in minimizing an objective function $f(x)$ (the cost, the volume ...) subject to a physical, geometrical or functional constraints:

$$\min_x f(x) \tag{26}$$

$$s.t\begin{cases}g_k(x)\le 0, & k=1\ldots K\\ h_j(x)=0, & j=1\ldots J\end{cases}$$

Where x is the vector of deterministic design variables, $g_k(x)$ are the inequality constraints and $h_j(x)$ are the equality constraints. Therefore, several methods and

https://doi.org/10.1017/jmech.2017.44 Published online by Cambridge University Press

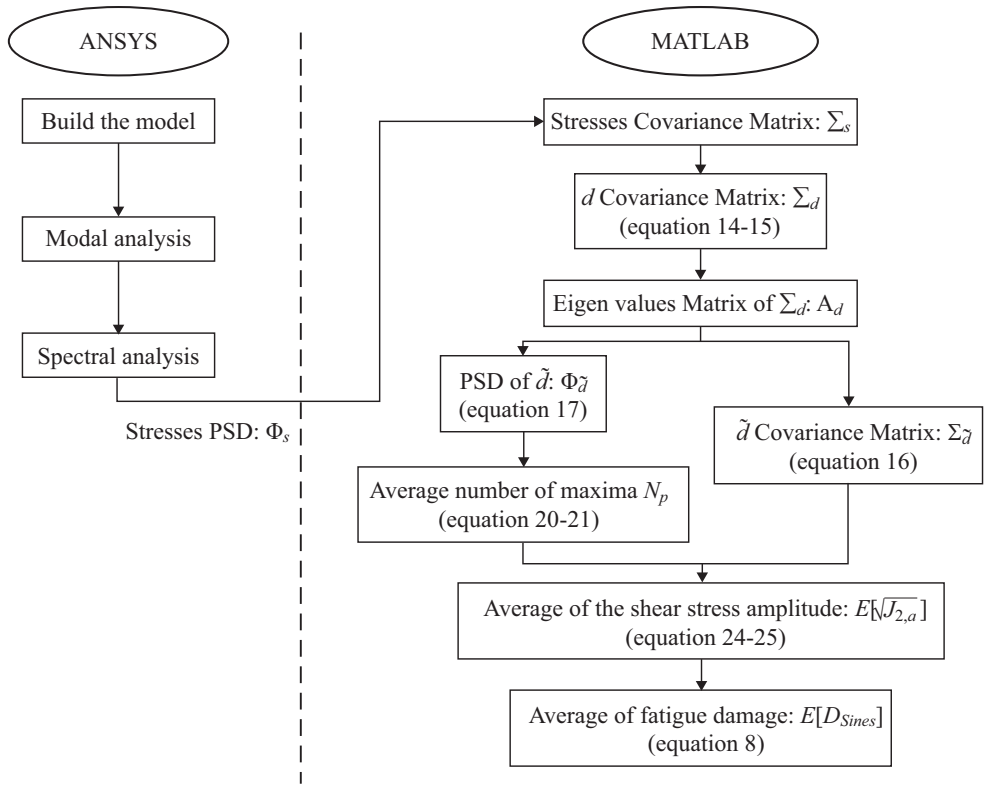


Fig. 1 Implementation of the fatigue damage analysis strategy.

algorithms have been treated in order to solve the DDO problem [31-34].

The DDO can offer an optimum design, but it cannot control the reliability level [27]. In other word, the true design's safety cannot be guaranteed by the chosen safety factors. To this end, the Reliability Based Design Optimization is necessary for optimal and reliable designs.

3.2 Reliability-Based Design Optimization RBDO

In the literature, several studies are treated in terms of RBDO [35-40]. An RBDO problem can be considered as an optimization problem subject to both deterministic and probabilistic constraints. It can be presented as a general form as following:

$$\min_x f(x) \tag{27}$$

$$s.t \begin{cases} P_r[G_i(x,y) \le 0] \le P_i^T, & i = 1 \ldots m \\ h_j(x) \le 0, & j = m+1 \ldots M \end{cases}$$

Where x is the vector of deterministic design variables, y is the vector of random variables. $P_r[.]$ is the probability operator, P_i^T is the target failure probability, G_i is the performance function and $h_j(x)$ is the deterministic constraints.

In an RBDO problem, the reliability index is calculated iteratively. To this end, solving an RBDO problem for such a design needs an enormous computing time. To reduce the computational time, an efficient method called hybrid method have been developed. It consists in solving simultaneously the reliability and the optimization problem [13]. for this purpose, the optimization problem become more complex than the deterministic optimization. To solve this problem a new method called Optimum Safety Factor (OSF) have been elaborated [14]. Using this method, the computing time have been reduced with a minimum of complexity compared to the hybrid method.

3.2.1 Classical Approach

Generally, using the classical approach, we use two spaces to perform the RBDO problem. These spaces are Physical Space and normalized space [41]. Consequently, the optimal solution is achieved by considering two nested problems:

i. Optimization problem

It consists in minimizing an objective function $f(x)$ subject to deterministic constraints $g_k(x)$ and the reliability exigence. It can be defined by:

$$\min_x f(x) \tag{28}$$

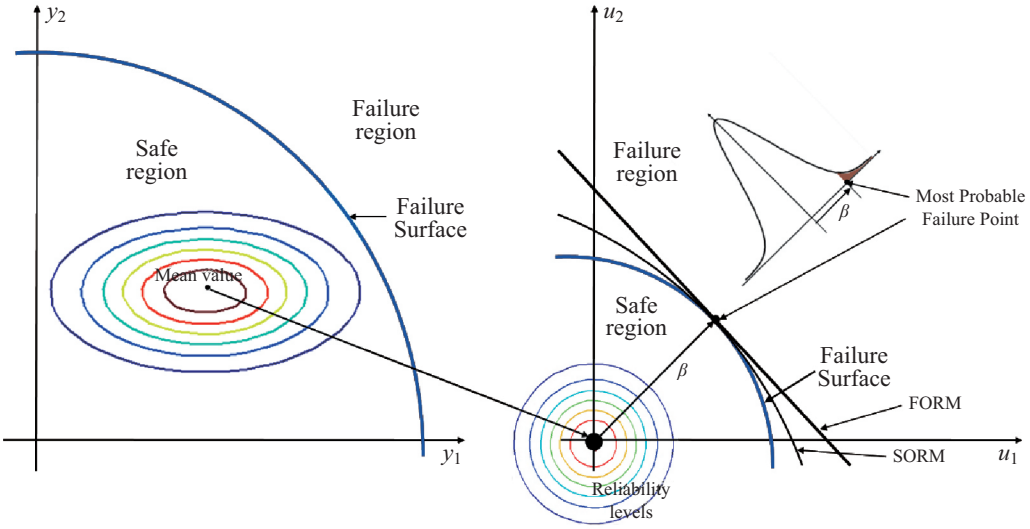
$$s.t \begin{cases} g_k(x) \le 0, & k = 1 \ldots K \\ \beta(x,u) \ge \beta_t \end{cases}$$

Where $\beta(x,u)$ is the reliability index of the structure and β_t is the target reliability index.

ii. Reliability problem

$\beta(x,u)$ represents the minimal distance between the origin and the limit state function $H(x,u)$ in the nor-

https://doi.org/10.1017/jmech.2017.44 Published online by Cambridge University Press



(a) Physical space (b) Normalized space

Fig. 2 Physical space and normalized space.

malized space; see Fig. 2a and Fig. 2b. It can be calculated by solving the following minimization problem:

$$\min d_\beta(u) = \sqrt{\Sigma u_i^2} \tag{29}$$

$$s.t\ H(x,u) \le 0$$

It has been proved that the classical approach need a high computational time by the reason of the high number of numerical calculation in the two spaces. In order to reduce the effects of this problem, an efficient approach called hybrid approach has been elaborated [13].

3.2.2 Hybrid Approach

In the hybrid approach, the objective function has a new form compared with the classical approach [13]. The minimization of this new objective function $F(x, y)$ is subject to the limit state function $G(x, y)$ and the deterministic constraints $g_k(x)$ as well as to the reliability constraint.

$$\min_{x,y} F(x,y) = f(x) \times d_\beta(x,y) \tag{30}$$

$$s.t \begin{cases} G(x,y) \le 0 \\ g_k(x) \le 0, \quad k = 1 \ldots K \\ \beta(x,u) \ge \beta_t \end{cases}$$

Here, $d_\beta(x,y)$ present the distance between the design point and the optimum one in the hybrid space. The minimization of the objective function is carried out in a hybrid design space (HDS). This HDS includes random variables y and deterministic variables x.

Figure 3 present an example of a HDS for a normal distribution of two random variables. In this figure, the objective function levels, the limit state function levels and the reliability levels d_β are presented. In addition, we can see two important point: the optimal solution point P_x^* and the design point P_y^* founded on the intersection of the curve $G(x, y) = 0$ and $d_\beta = \beta_t$. In the

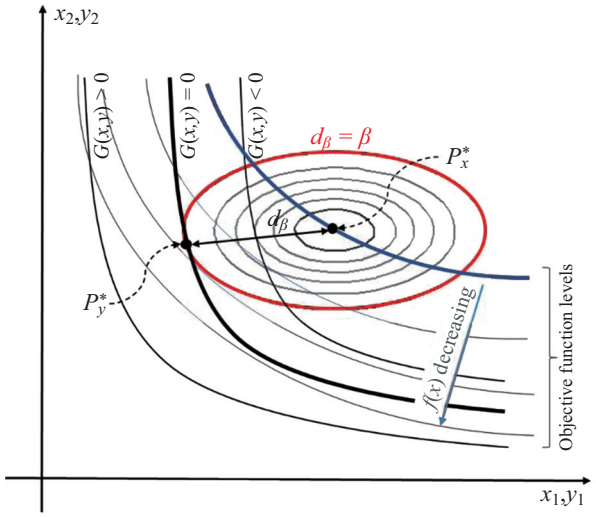


Fig. 3 Hybrid Design Space.

literature, the hybrid method has efficiently reduced the computing time comparing with the classical approach.

3.2.3 Optimum Safety Factor (OSF)

In the deterministic design optimization (DDO), the estimation of the safety factors is based on the engineering experience and the resulting solution can not satisfy the required reliability level. Then, when we design a new type of structure, we generally need some experimental background to provide an appropriate safety factors. However, with the OSF approach the determination of the safety factors should be independent of the engineering experience.

Although the hybrid method leads to improve the reliability level, with the OSF approach we leads to minimize the computational time. It consists in using the sensibility analysis combined with the reliability analysis in order to eliminate the disadvantages of the DDO method and the RBDO methods [42-43].

https://doi.org/10.1017/jmech.2017.44 Published online by Cambridge University Press

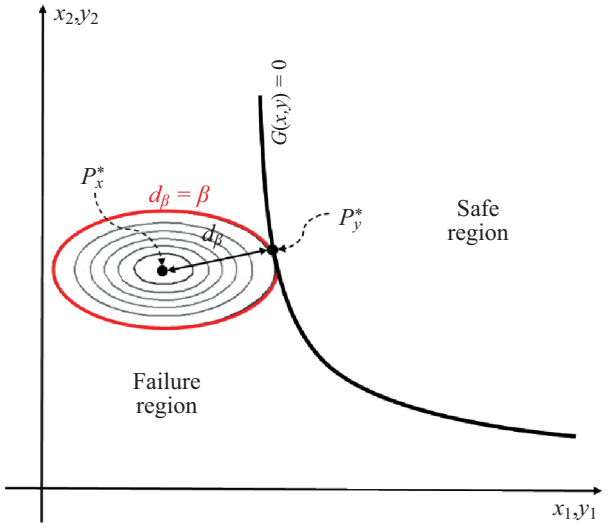


Fig. 4 Encountered problem of the classical Hybrid Method presented in the HDS.

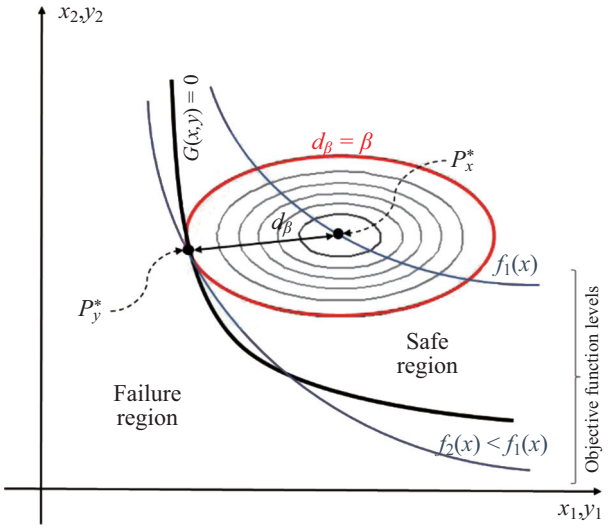


Fig. 5 RHM in the HDS.

The OSF algorithm is composed of three principal steps:

i. Determination of the design point y_i^* :

Here we minimize the objective function subject to the limit state function $G(y)$ and the deterministic constraints. The resulting solution is designed by the most probable failure point and is called the design point.

ii. Calculation of the safety factors:

In fact, the design point y_i^* is related with the optimal point x_i^* as defined in the Eq. (31). Here we consider that the mean values of random variable m_i are presented by the deterministic variable x_i. [44]

$$y_i^* = S_f^i x_i^*, \quad i = 1,\ldots,n \tag{31}$$

Furthermore, in general, for a normal distribution of the random variable y_i, we consider the transformation to the normalized space (u-space) from the physical space (x-space) as defined in the Eq. (32):

$$u_i = \frac{y_i - x_i}{\sigma_i}, \quad i = 1,\ldots,n \tag{32}$$

So the safety factor can be determined from u_i^* shown in Eq. (33) by combining the Eqs. (31) and (32).

$$S_f^i = 1 + \gamma_i u_i^*, \quad i = 1, \ldots, n \tag{33}$$

Where γ_i is a coefficient relating the mean with the standard-deviation: $\gamma_i = \dfrac{\sigma_i}{m_i}$

According to Kharmanda [17] the optimum value of the normalized vector u_i^* can be determined from the derivatives of the limit state function at the design point as follow:

$$u_i^* = \pm\beta_t \sqrt{\frac{\left|\dfrac{\partial G}{\partial y_i}\right|}{\Sigma_{j=1}^n \left|\dfrac{\partial G}{\partial y_j}\right|}}, \quad i = 1, \ldots, n \tag{34}$$

Where the ± sign depends on the sign of the derivative:

$$\frac{\partial G}{\partial y_i} > 0 \rightarrow u_i^* > 0 \text{ et } \frac{\partial G}{\partial y} < 0 \rightarrow u_i^* < 0, \quad i = 1,\ldots,n$$

iii. Calculation of the optimal solution:

In the final step, to determine the optimal design, we include the computed safety factors values in the design variables value.

4. ROBUST HYBRID METHOD (RHM)

In addition to the high computational time drawback of the classical Hybrid Method, it may converge to a non-feasible solution. In other words, the obtained optimal solution P_x^* may be located in the failure region ($G(x^*) > 0$) while the distance between the optimal point and the design point P_y^* gives an acceptable level of reliability, as shown in Fig. 4.

A new method called Robust Hybrid Method is then developed in order to solve this problem. It consists in adding another constraint, to force the optimization algorithm to find the optimal solution in the safe zone.

In fact, in the HDS, in order to guarantee the reliability of a structures under uncertainties, the value of the objective function at the optimal solution should be higher than that value at the design point. The Robust Hybrid Method can then be defined by Eq. (35):

$$\min_{x,y} F(x,y) = f(x) \times d_\beta(x,y) \tag{35}$$

https://doi.org/10.1017/jmech.2017.44 Published online by Cambridge University Press

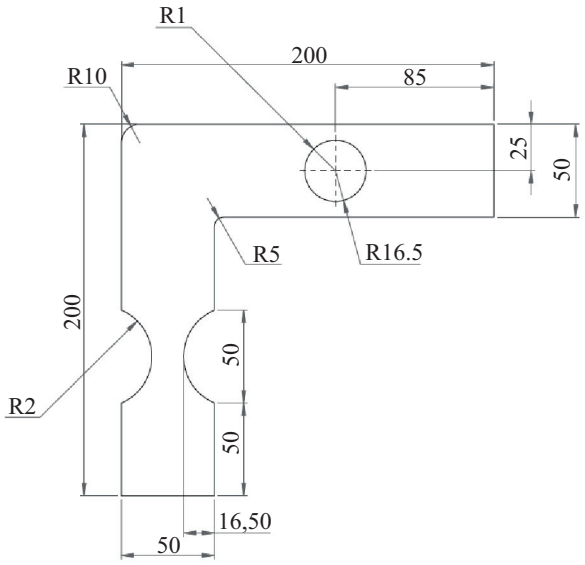


Fig. 6 Geometry.

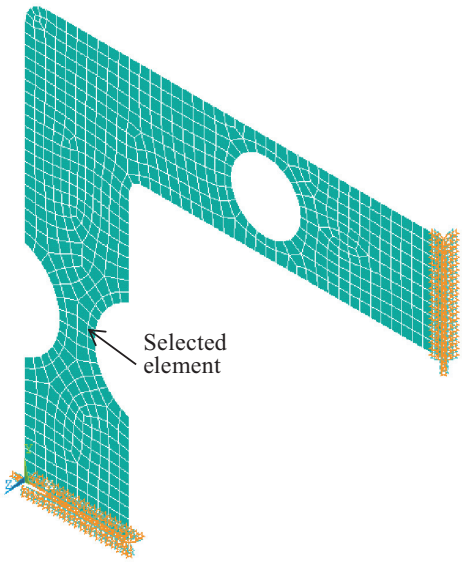


Fig. 7 Finite Element Model.

$$s.t\begin{cases} G(x,y) \le 0 \\ g_k(x) \le 0, \quad k = 1 \ldots K \\ \beta(x,u) \ge \beta_t \\ f(x) \ge f(y) \end{cases}$$

Figure 5 shows an example of the RHM presented in the Hybrid Design Space. $f_1(x)$ and $f_2(x)$ are two objective function levels which intersect respectively with the optimal point P_x^* and the design point P_y^*. It can be observed that the optimal point P_x^* is located in the safe region and $f(x^*) > f(y^*)$ and the required reliability level is also satisfied ($d_\beta = \beta_t$).

The proposed method does not only allow to force the optimization algorithm in the Hybrid Design Space but can also efficiently reduce the computational time comparing with the classical hybrid method.

5. NUMERICAL APPLICATION ON THE FATIGUE DAMAGE ANALYSIS

5.1 Problem Description

To illustrate the efficiency of the proposed fatigue damage analysis strategy, the simple plate illustrated in Fig. 6 is analyzed. This example is the same as that studied by Pitoiset [2] where Matake and Crossland criterion are applied.

The plate has a hole and a notch and its thickness is $e = 0.8mm$. It is clamped at both ends and each clamp is subjected to a band-limited white noise acceleration along the normal direction to the plate plane (z), ($\Phi_a = 4\ (\mathrm{m/s^2})^2/Hz$; $f_c = 400Hz$). The two support accelerations are uncorrelated.

The plate was discretized into a total number of 644 shell elements. Each element has four nodes with six degrees of freedom at each node (Fig. 7).

Figures 8a, 8b, 8c, 8d and 8e present the first five modes which are within the bandwidth of the excitation ($f_1 = 26.13Hz$; $f_2 = 101.88Hz$; $f_3 = 120.68Hz$; $f_4 = 274.42Hz$; $f_5 = 385.11Hz$).

The PSD matrix of the stress components is calculated at each finite element using a random vibration code. The Power Spectral Density $\Phi_{s_{xx}s_{xx}}$, $\Phi_{s_{yy}s_{yy}}$ and $\Phi_{s_{xy}s_{xy}}$ of the stresses are respectively shown in Figs. 9a, 9b and 9c, in one selected element (marked in Fig. 7).

Figure 10 shows the damage distribution caused by this stress calculated by the Sines criterion. This result is almost similar to that founded by the Crossland and Matake criteria [2]. The small difference between the results is caused by the meshing accuracy. The various procedures have been implemented in MATLAB toolbox used as postprocessor of the finite element software ANSYS.

The efficiency of this strategy has been verified and then it can be coupled with the RBDO methods in order to obtain the best design of the structure.

The current objective is to minimize the volume V of the piece under the fatigue damage constraint $D_{\max}$. The design variables are the radius R_1 of the hole the radius R_2 of the notch and the thickness e of the plate (see Fig. 6). These design variables are normally distributed and the variance coefficient γ of each variable is equal to 0.1. m_{R_1}, m_{R_2} and m_e are respectively the mean values of R_1, R_2 and e.

5.2 DDO and RBDO Procedures

Let's note $x = \{x_i\}_{i=1,2,3}$ the vector of deterministic design variables R_1, R_2 and e presented by its means ($x = \{m_{R_1}, m_{R_2}, m_e\}$) and y the vector of the random design variables ($y = \{R_1, R_2, e\}$). We can define also: the start point $x_0 = \{x_{i0}\}_{i=1,2,3} = \{R_{10}, R_{20}, e_0\}$, the design point $y^* = \{y_i^*\}_{i=1,2,3} = \{R_{1y}^*, R_{2y}^*, e_y^*\}$ and the optimal

https://doi.org/10.1017/jmech.2017.44 Published online by Cambridge University Press

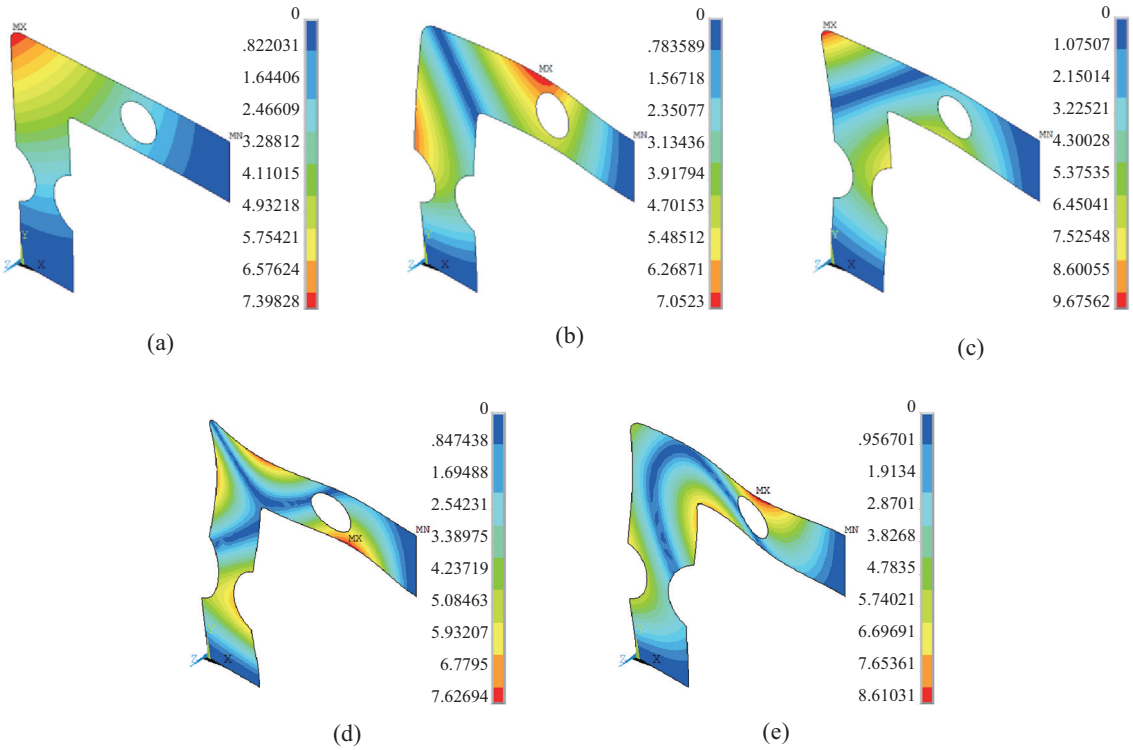


Fig. 8 Normal modes: (a) Mode 1 (b) Mode 2 (c) Mode 3 (d) Mode 4 (e) Mode 5.

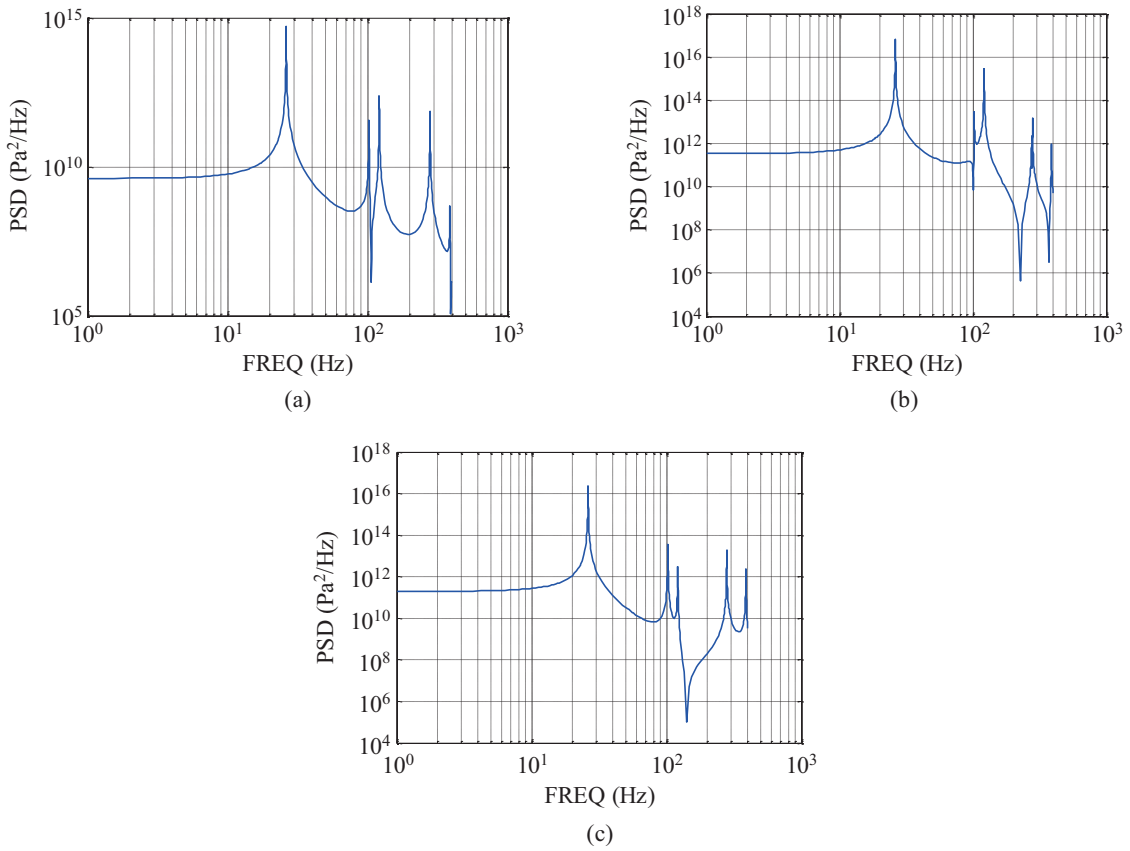


Fig. 9 Stresses Power Spectral Densities: (a) $\Phi_{s_{xx}s_{xx}}$ (b) $\Phi_{s_{yy}s_{yy}}$ (c) $\Phi_{s_{xy}s_{xy}}$

https://doi.org/10.1017/jmech.2017.44 Published online by Cambridge University Press

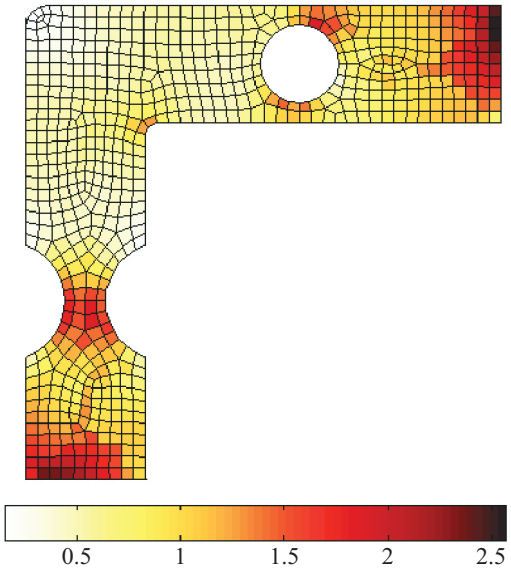


Fig. 10 Local value of damage of Sines criteria.

point $x^* = \{x_i^*\}_{i=1,2,3} = \{R_{1x}^*, R_{2x}^*, e_x^*\}$.

In the DDO approach, we consider a global safety factor S_f that is applied to the damage $D_{\max}$ and based on engineering experience. Thus, the optimal design of the structure should not exceed the maximum allowable values. Therefore, the structural optimization problem can be written as follows:

$$\min_x V(x) \tag{36}$$

$$s.t\ D_{\max}(x) \le D_w = 0.8$$

The DDO procedure does not contain the reliability constraint, that cannot control the reliability level. So, there is a strong need to the use the RBDO methods.

Using the Hybrid Method problem, which is presented in the Eq. (36), the objective function becomes a multiplication of the volume V by the distance in the hybrid design space as follow:

$$\min_{x,y} F(x,y) = V(x) \times d_\beta(x,y) \tag{37}$$

$$s.t \begin{cases} D_{\max}(y) \le 1 \\ d_\beta(x,y) \ge \beta_t \end{cases}$$

In addition to the fatigue limit state, the distance d_β should be superior or equal to the target reliability index β_t. In our case, β_t is equal to three which corresponds to a failure probability almost equal to 10^{-3}.

To overcome the problems of the classical hybrid method, the RHM is then applied. It consists in adding a third constraint to the optimization problem. The optimization problem of the robust hybrid method is then:

$$\min_{x,y} F(x,y) = V(x) \times d_\beta(x,y) \tag{38}$$

$$s.t \begin{cases} D_{\max}(y) \le 1 \\ d_\beta(x,y) \ge \beta_t \\ V(x) \ge V(y) \end{cases}$$

To obtain the optimal solution using OSF method, we should determine the design point at the first step. This design point is obtained by solving the optimization problem defined by the following formulation:

$$\min_y V(y) \tag{39}$$

$$s.t\ D_{\max}(y) \le 1$$

Then, as a second step, we calculate the safety factors from the derivatives of the limit state function $D_{\max}$. The optimal solution is then calculated by division of the design point values by the calculated safety factors.

5.3 Results and Discussions

In this section, we will show and compare the results of the different methods studied previously.

Table 1 presents the results of the DDO method. The optimal solution satisfies the constraint of the fatigue damage but the reliability level is less than the target reliability level β_t.

The hybrid method results are presented in Table 2. It can clearly be seen that the resulting optimal point is in the failure domain ($D_{\max} > 1$) while the distance between the optimal point and the design point β gives an acceptable level of reliability.

The results of the RHM are presented in Table 3. Note that the optimal solution is within the safety area and reliability level is verified. This change has also helped to minimize the computation time. In fact, the computational time of the new formulation is about 8 hours while conventional hybrid method for computing time is about 27 hours with no feasible result found. The efficiency of this new formulation is then shown.

https://doi.org/10.1017/jmech.2017.44 Published online by Cambridge University Press

Table 1 DDO results

		Initial values x_0	Design point y^*	Optimal solution x^*
Design variables	R_1	15	17	16.53
	R_2	22	24.12	22.37
	e	2	0.96	1.06
Objective function	V	31 868.82	14 911.01	16757.96
Optimization constrain	$D_{\max}$	0.137	1	0.799
	β			1.27

Table 2 Hybrid method Results

		Distribution	Initial values y_0	Initial values x_0	Design point y^*	Optimal solution x^*
Design variables	R_1	Normal	16.5	15	16.58	17
	R_2	Normal	25	22	25.98	26
	e	Normal	0.8	2	1.17	0.9
Objective function	V		12357.91	31 868.83	17957.41	13782.28
Optimization constrain	$D_{\max}$		2.564	0.1372	1.0001	2.3458
	β			6.2337		3

Table 3 Robust hybrid method Results

		Distribution	Initial values y_0	Initial values x_0	Design point y^*	Optimal solution x^*
Design variables	R_1	Normal	16.5	16	17	14.16
	R_2	Normal	25	21	26	21.36
	e	Normal	0.8	1.5	1.16	1.11
Objective function	V		12357.91	23905.73	17829.22	17829.22
Optimization constrain	$D_{\max}$		2.564	0.272	1	0.77
	β			5.05		3

Table 4 OSF Results

		Distribution	Initial values x_0	Design point y^*	Normalized variable u^*	OSF S_f	Optimal solution x_i^*
Design variables	R_1	Normal	15	17	0.2271	1.023	16.62
	R_2	Normal	22	24.12	0.2009	1.02	23.64
	e	Normal	2	0.962	-2.9846	0.7	1.37
Objective function	V		31 868.82	14 911.01			21 384.57
Optimization constrain	$D_{\max}$		0.1372	1.0001			0.36
	β						3

Table 4 shows the results of the OSF method. To find these results a sensitivity analysis is required to show the influence of various parameters on the maximum fatigue damage. Table 5 defines the sensitivity (derivatives) of the maximum fatigue damage with respect to different design variables.

With the OSF method, the computational time is approximately 7 hours. This method allowed to minimize the computing time compared to the DDO method and the hybrid method. However, it is negligible com-

https://doi.org/10.1017/jmech.2017.44 Published online by Cambridge University Press

Table 5 Sensibility analysis of the maximum of the fatigue damage

$\frac{\partial D_{\max}}{\partial R_1}$	$\frac{\partial D_{\max}}{\partial R_2}$	$\frac{\partial D_{\max}}{\partial e}$
0.017	0.013	-2.993

Table 6 Initial points for the RHM method

		Point 1	Point 2	Point 3	Point 4	Point 5	Point 6
x_0	R_{10}^x	16	14	16	16	17	16
	R_{20}^x	21	26	21	21	21	20
	e_0^x	1.5	1.8	1.5	1.5	1.3	0.7
	V_{x_0}	23905.73	28010.47	23905.73	23905.73	20583.53	11221.6
	$D_{\max}^{x_0}$	0.29	0.32	0.29	0.29	0.41	2.55
y_0	R_{10}^y	16.5	17	17	16.5	17	15
	R_{20}^y	25	24	24	25	23	22
	e_0^y	0.8	0.6	0.6	0.8	0.8	1.2
	V_{y_0}	12357.91	9308.38	9308.38	12357.91	12501.47	19121.29
	$D_{\max}^{y_0}$	2.56	3.74	3.74	2.56	1.75	0.53

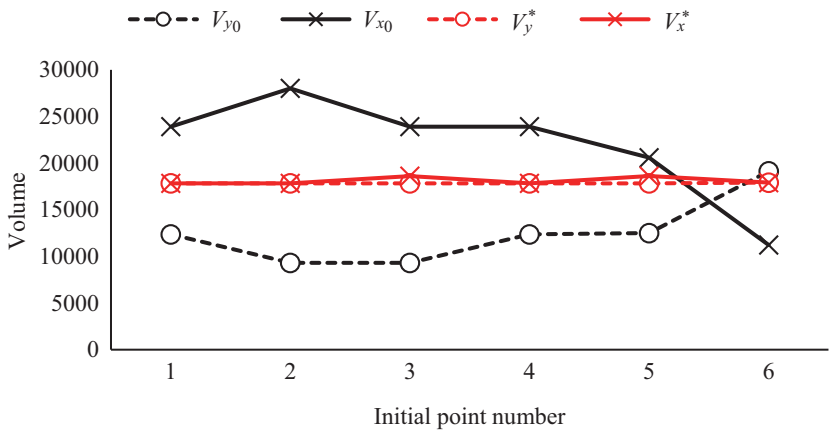


Fig. 11 objective function values at the initial and optimal points for different initial point.

pared to the robust hybrid method. In addition, the value of the objective function of the optimal point obtained by the robust hybrid method is less than that founded by the OSF method ($V_{OSF}^* > V_{RHM}^*$).

To verify the efficiency of the RHM when changing the initial point, the optimization problem has been solved with different initial points. It was found that, in most cases, the RHM optimization converges to a feasible solution. Table 6 presents different initial points where the program is converged. It should be mentioned that those points are chosen arbitrary.

Figure 11 presents the initial objective functions V_{x_0} and V_{y_0} (black curves) and the optimal objective functions V_x^* and V_y^* (red curves) calculated for each initial point. A brief analysis of this result points out that the RHM optimization problem converges almost to the same optimal point (see the red curve in Fig. 11). It can be concluded that the RHM is an efficient and robust method and can lead to the same optimal solution when considering different initial points.

As a result, the robust hybrid method provides the best results as compared to other methods, when solving an RBDO problem of structures under random vibrations. It can overcome the shortages of lack of reliability level for the DDO model and avoid the fault that the optimal point falls within the failure region. Furthermore, no more computational time is needed when compared with the OSF method. Let's study now the influence of the excitation on the optimal solution. More specifically,

https://doi.org/10.1017/jmech.2017.44 Published online by Cambridge University Press

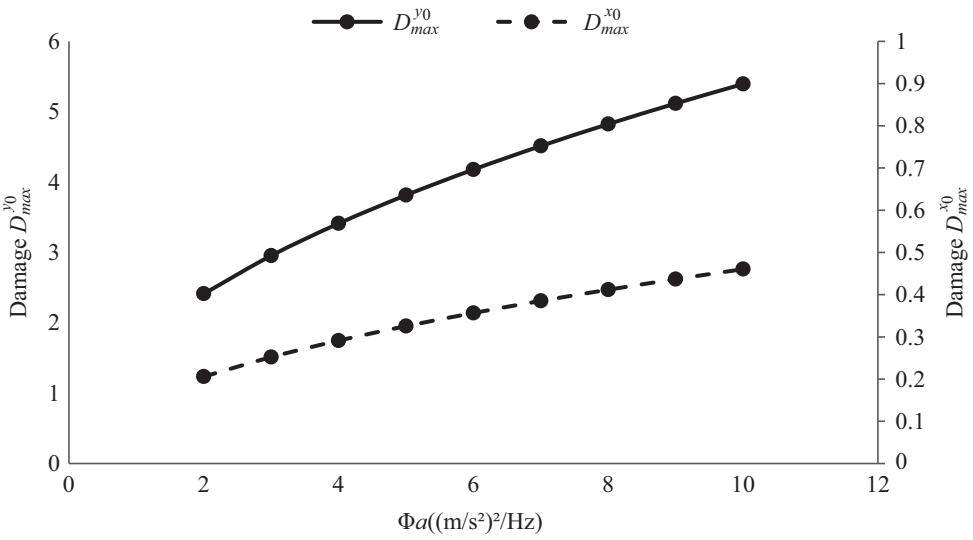


Fig. 12 Influence of the excitation value on the fatigue damage at the initial point.

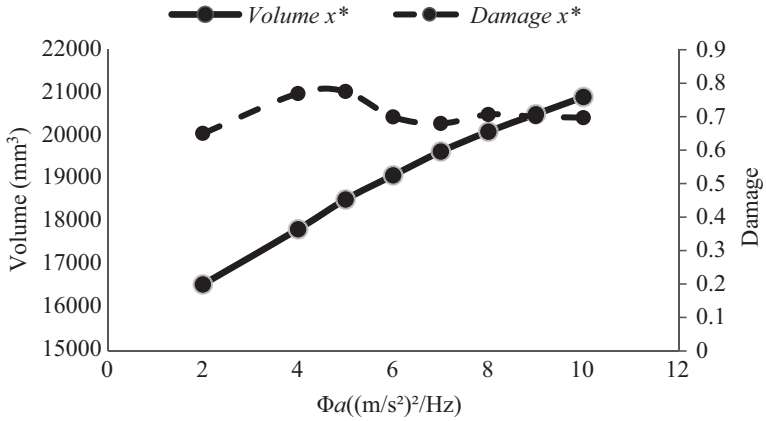


Fig. 13 Influence of the excitation on the objective function and the constrain at the optimal point.

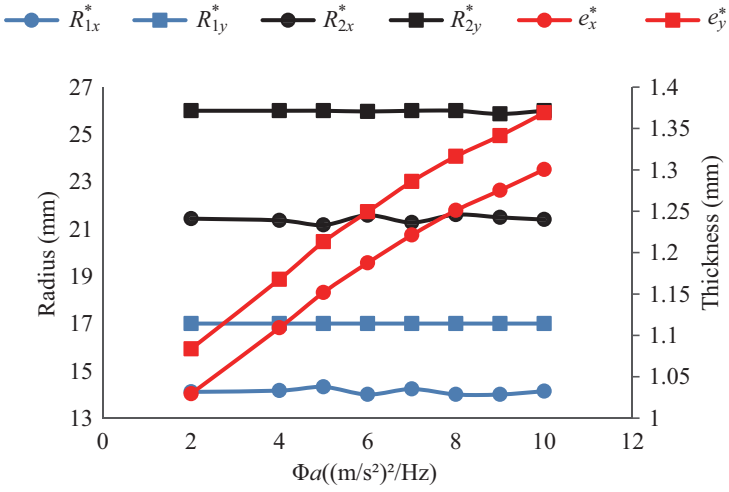


Fig. 14 Influence of the excitation on the design variables.

https://doi.org/10.1017/jmech.2017.44 Published online by Cambridge University Press

we study the impact of the value of the white noise PSD of the excitation Φ_a on the design point for the same example studied previously.

Figure 12 shows the influence of the excitation value on the maximum of the fatigue damage at the chosen initial point. It can be observed that the maximum value of the fatigue damage increases when the excitation PSD value increases.

Figure 13 present the variation of the volume and the maximal of the fatigue damage at the optimal point as a function of the excitation PSD. This figure shows that the optimal volume of the structure should increase if the PSD of the excitation value increases. However, it can be observed that the maximal fatigue damage of the optimal design is nearly the same for all configurations and it does not change if the excitation value changes. It can be noted that, at each obtained optimal point, the reliability of the optimum design is respected $\beta = \beta_t$.

The variation of the design variables as a function of the excitation PSD is presented in Fig. 14. The design variables of the optimal point x^* are presented by a solid circle and the optimization variables of the design point y^* are presented by a solid square, for each variation of the excitation PSD. The blue lines present the variation of the radius of the hole R_1, the black lines present the variation of the radius of the notch and the red lines present the thickness variation. It can be observed that the optimal radiuses don't change if the excitation PSD changes. However, the optimal thickness of the plate increases if the PSD increases.

It can be concluded that the volume variation for each PSD (see Fig. 10) is caused by the variation of the thickness. Also, the shape of the thickness curve is similar to the shape of the volume curve.

6. CONCLUSIONS

In this paper, our aim is to develop an efficient method that allows us to obtain an optimal design of structures subject to random vibration that can guarantee a required structural reliability level considering fatigue damage. Therefore, we first demonstrate that the DDO is easy to implement and it can guarantee an optimum design but it cannot control the reliability level. Next, RBDO methods such as the hybrid method and the OSF method are applied. Comparing with the DDO model, the RBDO model respects a required reliability level. Using the hybrid method, the obtained design point is within the failure region and the result is then rejected. For this purpose, a new method called Robust Hybrid Method (RHM) is then proposed. An application on a structure subjected to random vibration with the fatigue damage as the optimization constraint, demonstrated that the optimal solution founded by the RHM is more reliable than the classical hybrid method and DDO the method. Using the RHM, the obtained objective function is less than that obtained by the OSF method. In addition, the computational time of the RHM is almost the same as the OSF method. The efficiency of the new method is then demonstrated.

REFERENCES

1. Pitoiset, X. and Preumont, A., "Spectral Methods for Multiaxial Random Fatigue Analysis of Metallic Structures," *International Journal of Fatigue*, **22**, pp. 541-550 (2000).
2. Pitoiset, X., Rychlik, I. and Preumont, A., "Spectral Methods to Estimate Local Multiaxial Fatigue Failure for Structures Undergoing Random Vibrations," *Fatigue Fract Engng Mater Struct*, **2**4, pp. 715-727 (2001).
3. Weber, B., Labesse-Jied, F. and Robert, J., "Comparison of Multiaxial High Cycle Fatigue Criteria and Their Application to Fatigue Design of Structures," *Sixth International Conference on Biaxial/Multiaxial Fatigue and Fracture*, Lisbon (2001).
4. Wu, B., Ferraton, L., Robin, C., Mesmacque, G. and Zakarzewski, D., "Application de Critère de Fatigue Multiaxiale Aux Sturctures en Alliage D'aluminum," *Conference of G2RT, TILT* (2003).
5. Pitoiset, X., "Méthodes Spectrales Pour une Analyse en Fatigue des Structures Métallique Sous Chargements Aléatoires Multiaxiaux," PhD. Dissertation, Université Libre de Bruxelles, Bruxelles (2001).
6. Chang, T. P. and Liu, M. F., "Evaluation of Nonlinear System Parameters by Stochastic Spectral Method," *Journal of Mechanics*, **23**, pp. 269-274 (2007).
7. Arora, J., *Introduction to Optimum Design*, McGraw-Hill, New York (1989).
8. Haftaka, R. and Gurdal, Z., *Elements of Structural Optimization*, Kluwer Academic Publications, Dordrecht (1991).
9. Kusano, I., Baldomir, A., Jurado, J. A. and Hernández, S., "Reliability Based Design Optimization of Long-Span Bridges Considering Flutter," *Journal of Wind Engineering and Industrial Aerodynamics*, **135**, pp. 149-162 (2014).
10. Makhloufi, A., Aoues, Y. and El Hami, A., "Reliability Based Design Optimization of Wire Bonding in Power Microelectronic Devices," *Microsystem Technologies*, **22**, pp. 2737-2748 (2016).
11. Xia, B. and Yu, D., "Optimization Based on Reliability and Confidence Interval Design for the Structural-Acoustic System with Interval Probabilistic Variables," *Journal of Sound and Vibration*, **336**, pp. 1-15 (2014).
12. Aoues, Y. and Chateauneuf, A., "Benchmark Study of Numerical Methods for Reliability-Based Design Optimization," *Struct Multidisc Optim*, **41**, pp. 277-294 (2010).
13. Kharmanda, G., Mohamed, A. and Lemaire, M., "Efficient Reliability Based Design Optimization Using a Hybrid Space with Application to Finite Element Analysis," *Struct Multidiscip Optim*, **24**, pp. 233-245 (2002).
14. Kharmanda, G., Sharabaty, S., Ibrahim, H., Mak-

https://doi.org/10.1017/jmech.2017.44 Published online by Cambridge University Press

hloufi, A. and El-Hami, A., "Reliability-Based Design Optimization Using Semi-Numerical Methods for Different Engineering Applications," *International Journal of CAD/CAM*, **9**, pp. 1-16 (2009).

15. Mohsine, A. and El Hami, A., "A Robust Study of Reliability-Based Optimization Methods under Eigen-Frequency," *Computer Methods in Applied Mechanics and Engineering*, **199**, pp. 1006-1018 (2010).
16. Kharmanda, G., *Numerical and Semi-Numerical Methods for Reliability-Based Design Optimization*, Structural Design Optimization Considering Uncertainties, Taylor & Francis e-Library, pp. 189-216 (2008).
17. Kharmanda, G., Ibrahim, M., Abo Al-kheer, A., Guerin, F. and El-Hami, A., "Reliability-Based Design Optimization of Shank Chisel Plough Using Optimum Safety Factor Strategy," *Computers and Electronics in Agriculture*, **109**, pp. 162-171 (2014).
18. Crossland, B., "Effect of Large Hydrostatic Pressures on the Torsional Fatigue Strength of an Alloy Steel," *Proceeding of International Conference on Fatigue of Metals*, **1**, pp. 138-149 (1956).
19. Sines, G., *Behaviour of Metals under Complex Static and Alternationg Stress*, McGraw-Hill, New York, pp. 145-169 (1959).
20. Weber, B., "Fatigue Multiaxiale des Structures Industrielles Sous Chargement Quelconque," PhD. Dissertation, INSA de Lyon, Lyon (1999).
21. Lambert, S., Pagnacco, E. and Khalij, L., "A Probabilistic Model for the Fatigue Reliability of Structures under Random Loadings with Phase Shift Effects," *International Journal of Fatigue*, **32**, pp. 463-474 (2010).
22. Li, B. and Freitas, M., "A Procedure for Fast Evaluation of High-Cycle Fatigue under Multiaxial Random Loading," *Journal of Mechanical Design*, **124**, pp. 558-563 (2002).
23. Balthazar, J. and Malcher, L., *A Review on the Main Approaches for Determination of the Multiaxial High Cycle Fatigue Strengh*, Marcilio Alves & da costa Mattos, Brazil (2007).
24. Bernasconi, A., "Efficient Algorithms for Calculation of Shear Stress Amplitude and Amplitude of the Second Invariant of the Stress Deviator in Fatigue Criteria Applications," *International Journal of Fatigue*, **24**, pp. 649-657 (2002).
25. Papuga, J., "Mapping of Fatigue Damages Program Shell of FE-Calculation," PhD. Dissertation, Faculty of Mechanical Engineering, Prague (2005).
26. Cristofori, A., Susmel, L. and Tovo, A., "A Stress Invariant Based Criterion to Estimate Fatigue Damage under Multiaxial Loading," *International Journal of Fatigue*, **30**, pp. 1646-1658 (2008).
27. Liu J. and Zenner, H., "Fatigue Llimit of Ductile Metals under Multiaxial Loading," *Biaxial/Multiaxial Fatigue and Fracture, 6 International Conference on Biaxial/Multiaxial Fatigue and Fracture*, Elsevier, Lisbon, Portugal, **31**, pp. 147-164 (2003).
28. Gonçalves, C., Araujo, J. and Mamiya, E., "A Simple Multiaxial Fatigue Criterion for Metals," *Comptes Rendus Mécanique*, **332**, pp. 963-968 (2004).
29. Zouain, N., Mamiya, E. and Comes, F., "Using Enclosing Ellipsoids in Multiaxial Fatigue Strength Criteria," *European Journal of Mechanics - A/Solids*, **25**, pp. 51-71 (2006).
30. Davenport A. G., "Note on the Distribution of Largest Values of Random Function with Application to Gust Loading" *Proceedings of the Institution of Civil Engineers*, **28**, pp. 187-196 (1964).
31. Arora, J. S., *Introduction to Optimum Design*, Second Edition, Elsevier, Amsterdam (2004).
32. Bhatti, M. A., *Practical Optimization Methods with Mathematical Applications*, Springer-Verlag, New York (2000).
33. Lange, K., *Optimization*, Springer-Verlag, New York (2004).
34. Pedregal, K., *Introduction to Optimization*, Springer-Verlag, New York (2004).
35. Stevenson, J., *Reliability Analysis and Optimum Design of Structural Systems with Applications to Rigid Frames, Division of Solid Mechanics and Structures*, **14**, Case Western Reserve University, Cleveland, Ohio (1967).
36. Moses, F., "Structural System Reliability and Optimization," *Comput Struct*, **7**, pp. 283-290 (1977).
37. Feng, Y. and Moses, F., "A Method of Structural Optimization Based on Structural System Reliability," *Journal of Structural Mechanics*, **14**, pp. 437-453 (1986).
38. Chandu, S. and Grandhi, R., "General Purpose Procedure for Reliability Structural Optimization under Parametric Uncertainties," *Advances in Engineering Software*, **23**, pp. 7-14 (1995).
39. Du, X. and Chen, W., "Sequential Optimization and Reliability Assessment Method for Efficient Probabilistic Design," *Journal of Mechanical Design,* **126**, pp. 225-233 (2004).
40. Steenackers, G., Versluys, R., Runacres, M. and Guillaume, P., "Reliability-Based Design Optimization of Computation-Intensive Models Making Use of Response Surface Models," *Quality and Reliability Engineering International*, **27**, pp. 555-568 (2011).
41. Lemaire, M., *Fiabilité des Structures*, HERMES-LAVOISIER, Paris, p. 506 (2005).
42. Kharmanda, G., Olhoff, N. and El-Hami, A., "Optimum Values of Structural Safety Factors for a Predefined Reliability Level with Extension to Multiple Limit States," *Structural and Multidisciplinary Optimization*, **27**, pp. 421-434 (2004).
43. Kharmanda, G. and Olhoff, N., "Extension of Opti-

https://doi.org/10.1017/jmech.2017.44 Published online by Cambridge University Press

mum Safety Factor Method to Nnonlinear Reliability-Based Design Optimization," *Journal of Structural and Multidisciplinary Optimization*, **43**, pp. 367-380 (2007).

44. Lopez, R. H., Lemosse, D., Cursi, E. S., Rojas, J. E. and El-Hami, A., "An Approach for the Reliability Based Design Optimization of Laminated Composite Plates," *Engineering Optimization*, **43**, pp. 1079-1094 (2011).

(Manuscript received November 11, 2016, accepted for publication May 25, 2017.)

https://doi.org/10.1017/jmech.2017.44 Published online by Cambridge University Press